# Real Wastewater Treatment Using a Moving Bed and Wastewater-Borne Algal?Bacterial Consortia with a Short Hydraulic Retention Time

*Authors:*

Donghan Kang, Keugtae Kim

*Abstract:*

Algal?bacterial consortium is a promising technology, combined with wastewater treatment plants, because algae produce molecular oxygen for nitrification and organic removal and reduce carbon dioxide emissions. However, algal?bacterial consortia based on suspended growth require a relatively long hydraulic retention time (HRT) of 4 d to 6 d for removal of organic matter and nutrients. For the algal?bacterial consortia in a photobioreactor (PBR) containing a moving bed, the organic matter and nutrient removal and the community structure of algal?bacterial consortia were investigated to determine the performance under a relatively short HRT of 2.5 d. Moving media containing algal?bacterial consortia enhanced the photosynthetic oxygen concentration (0.2 mg dissolved oxygen (DO)·L?1 to 5.9 mg DO·L?1), biochemical oxygen demand removal (88.0% to 97.2%), ammoniacal nitrogen removal (33.8% to 95.3%), total nitrogen removal (61.6% to 87.7%), total phosphate removal (66.4% to 88.7%), algal growth (149.3 mg algae·L?1 to 285.4 mg algae·L?1), and settleability (algae removal efficiency of 20.6% to 71.2%) compared with those of a PBR without moving media (SPBR). Although biomass uptake was the main mechanism for nutrient removal in the SPBR, both biomass uptake and denitrification were the main mechanisms in the PBR with moving media (MBPBR). The bacterial community also changed under the moving media condition. This study shows that moving media might be an essential parameter for PBRs with a short HRT to enhance nutrient removal and settleability.

*Article*

# Real Wastewater Treatment Using a Moving Bed and Wastewater-Borne Algal–Bacterial Consortia with a Short Hydraulic Retention Time

**Donghan Kang [1] and Keugtae Kim [2],\***

[1] Water Chemistry Team, Gyeonggi-do Institute of Health & Environment, 62, Chilbo-ro 1beon-gil, Gwonseon-gu, Suwon-si, Gyeonggi-do 16381, Korea; camoneys@gg.go.kr

[2] Department of Environmental & Energy Engineering, Suwon University, 17 Wauan-gil, Bongdam-eup, Hwasung-si, Gyeonggi-do 18323, Korea

\* Correspondence: kkt38@suwon.ac.kr; Tel.: +82-31-229-8355; Fax: +82-31-220-2533

**Abstract:** Algal–bacterial consortium is a promising technology, combined with wastewater treatment plants, because algae produce molecular oxygen for nitrification and organic removal and reduce carbon dioxide emissions. However, algal–bacterial consortia based on suspended growth require a relatively long hydraulic retention time (HRT) of 4 d to 6 d for removal of organic matter and nutrients. For the algal–bacterial consortia in a photobioreactor (PBR) containing a moving bed, the organic matter and nutrient removal and the community structure of algal–bacterial consortia were investigated to determine the performance under a relatively short HRT of 2.5 d. Moving media containing algal–bacterial consortia enhanced the photosynthetic oxygen concentration (0.2 mg dissolved oxygen (DO)$\cdot$L$^{-1}$ to 5.9 mg DO$\cdot$L$^{-1}$), biochemical oxygen demand removal (88.0% to 97.2%), ammoniacal nitrogen removal (33.8% to 95.3%), total nitrogen removal (61.6% to 87.7%), total phosphate removal (66.4% to 88.7%), algal growth (149.3 mg algae$\cdot$L$^{-1}$ to 285.4 mg algae$\cdot$L$^{-1}$), and settleability (algae removal efficiency of 20.6% to 71.2%) compared with those of a PBR without moving media (SPBR). Although biomass uptake was the main mechanism for nutrient removal in the SPBR, both biomass uptake and denitrification were the main mechanisms in the PBR with moving media (MBPBR). The bacterial community also changed under the moving media condition. This study shows that moving media might be an essential parameter for PBRs with a short HRT to enhance nutrient removal and settleability.

**Keywords:** microalgae; moving media; photobioreactor; bacterial community

## 1. Introduction

Advanced bioreactor design and operation in wastewater treatment plants (WWTPs) is essential for the safe and economic discharge of municipal wastewater. The main operating cost of WWTPs is associated with aeration, as it is required for both oxygen transfer and mixing. The aeration step alone accounts for 45–75% of the energy consumption of wastewater treatment [1,2].

The concept of algal–bacterial consortia has been particularly attractive for wastewater treatment over the past few years because they produce molecular oxygen that is used for nitrification and microbial decomposition of organic matter; consequently, the bacteria-produced $CO_2$ promoting microalgal growth [3–5]. In particular, this system provides a cheaper and safer alternative to mechanical aeration and contributes to $CO_2$ mitigation [6]. Recently, sequencing batch reactors (SBRs) have mostly been used to create such algal–bacterial systems [5,7].

As the hydraulic retention time (HRT) generally controls the nutrient loading and the solids retention time (SRT) controls the microbial growth rate [8], strategies used with SBRs, such as a short HRT coupled with a long SRT by recycling settleable flocs, have provided

a selective process to achieve the greatest productivity and settleability of algal–bacterial consortia [9]. A longer HRT requires a larger wastewater treatment system volume, which is the disadvantage of that system. The HRT is an important design parameter in the construction of algal–bacterial systems for wastewater treatment [10]. Algae growth is favored by short HRTs and high loading because they are in their logarithmic growth phase under such conditions, whereas under longer HRTs, algae reach their steady growth phase in which they still multiply, but slower, and their daughter cells are smaller [5]. For the microalgal–bacterial process, an HRT of 2 d to 6 d is suggested to operate high-rate algal ponds and enclosed photobioreactors (PBRs) [11–13]. However, when PBRs containing municipal wastewater were operated at HRTs of 2.0 d and 2.5 d, the algal–bacterial consortia system showed the lowest performance, such as low efficiencies of organic matter and nutrient removal and settling properties, whereas high chemical oxygen demand (>92%), ammonium (>85%), and phosphorus (up to 56%) removal were observed at HRTs of 4.0, 6.0, and 10.0 d [14,15]. In addition, shorter HRTs such as 2.0 d and 2.5 d generally resulted in lower dissolved oxygen (DO) owing to greater oxygen demand for wastewater degradation at higher loading rates [9]. Although some studies have been conducted to achieve good performance, such as high photosynthetic oxygen production, high organic matter and nutrient removal, and good settleability, there is scarce information on algal–bacterial consortia systems showing good performance under an HRT of 2.5 d [16–18]. Meanwhile, algal–bacterial consortia based on suspended growth with a relatively long HRT such as 4 d, 6 d, or greater enhanced the removal of organic matter and nutrients from wastewater [16–18]. A longer HRT would cause a longer SRT, which results in good performance. However, a process operated with short HRT and long SRT has been required for cost-effective wastewater treatment. In this respect, growing microalgae in attached non-suspended systems is an attractive and promising method because of its higher biomass yields, ease of scale-up, and better control of contamination compared with those of ordinary suspended PBRs [19]. Biofilm processes, especially moving bed biofilm reactors, are highly effective biological treatment processes that were developed on the basis of the conventional activated sludge process and biofilter process [20]. These biofilm reactors are especially useful when slow-growing organisms such as nitrifiers must be kept in a wastewater treatment process [21]. However, all the above studies focused on bacteria-based biofilms. Although there are many beneficial aspects of the biofilm process, few studies have reported the growth of microalgae on the surface, especially in a moving bed under a non-enclosure mode, and limited studies have been reported on the enclosure mode of attached non-suspended systems [19]. Therefore, in this study, a moving bed was applied to the PBR to obtain a long SRT capable of maintaining large populations of nitrifying bacteria and micro algae for nitrification and oxygen production, respectably. The potential of using moving bed-containing PBRs (MBPBRs) for the treatment of real wastewater was investigated using wastewater-borne algal–bacterial consortia in the absence of additional nutrients and inoculum to examine the properties of photosynthetic oxygen production, nutrient removal, and sedimentation under a short HRT (2.5 d).

## 2. Materials and Methods

### 2.1. Induction of Algal–Bacterial Consortia

The wastewater was collected from the overflow of a primary sedimentation tank in a domestic WWTP located in Yongin, Republic of Korea. It contained $210.5 \pm 62.0$ mg·L$^{-1}$ suspended solids, $62.7 \pm 6.0$ mg·L$^{-1}$ total nitrogen (TN), $62.3 \pm 6.0$ mg·L$^{-1}$ total Kjeldahl nitrogen (TKN), $31.5 \pm 3.4$ mg·L$^{-1}$ ammoniacal nitrogen (NH3-N), $0.3 \pm 0.3$ mg·L$^{-1}$ NOx–N (the sum of $NO_2^-$-N and $NO_3^-$-N), and $6.7 \pm 1.2$ mg·L$^{-1}$ total phosphate (TP); biochemical oxygen demand (BOD) was $248.5 \pm 55.3$ mg·L$^{-1}$ and alkalinity (as $CaCO_3$) was $217.5 \pm 14.0$ mg·L$^{-1}$. To culture wastewater-borne algal–bacterial consortia, raw wastewater was added to a PBR with a 12.5 L effective volume and irradiated at a rate of 500 µmol·m$^{-2}$·s$^{-1}$ for 24 h at 25 °C from one side of the reactor with a white light emitting diode (LED) stick (50 W; Sungkwang Co., Ltd., Suwon, Korea) (Figure 1).

After the second day, 40% of the effective volume was discharged for 10 min and the PBR was refilled with fresh raw wastewater for the same period. The mixed liquor was irradiated at 500 µmol·m$^{-2}$·s$^{-1}$ for 1420 min and agitated at 150 rpm. To summarize, the reactors were operated in photo-sequencing batch reactor (PSBR) mode every day with 10 min of filling, 1420 min of reaction time, and 10 min of withdrawal. After 2 months of cultivation, the algal–bacterial consortia were stabilized at 400 ± 15 mg·L$^{-1}$ of total suspended solid (TSS) and a pH of 7.2 ± 0.5. The algal–bacterial consortia grown in the induction culture were used to analyze the performances of two types of PBRs.
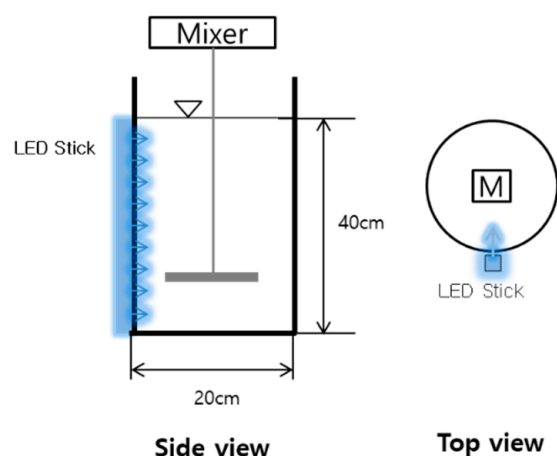


**Figure 1.** Schematic diagram of the induction photo bioreactor (photo-sequencing batch reactor—PSBR) used in this study.

### 2.2. MBPBR–SPBR Configuration and Experimental Process

The experiment was conducted using two PBRs. Each reactor was made of an acrylic cylinder with an internal diameter of 20 cm, height of 50 cm, and total volume of 16.0 L and mechanically agitated using an impeller speed at 200 rpm (Figure 2). One PBR was filled with moving media made of polyurethane (15 mm × 15 mm × 15 mm) (MBPBR), and the other PBR was not filled with moving media (SPBR). Both the MBPBR and SPBR with working volumes of 12.5 L were illuminated by an LED with white light. For the light intensity of 500 µmol·m$^{-2}$·s$^{-1}$, one LED stick was placed at one side of both reactors. In the MBPBR, a moving medium with a specific gravity of 0.04, specific surface area of 4000 m$^2$·m$^{-3}$, and porosity of 95% was filled with a 5% packing fraction.
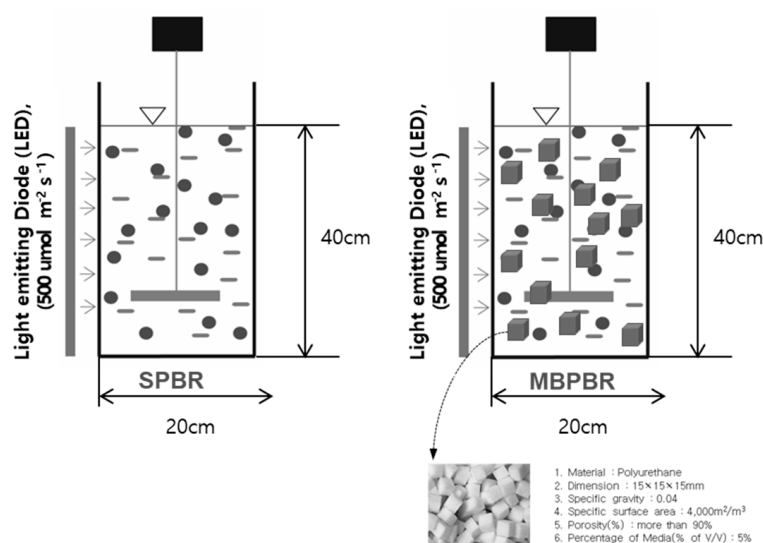


**Figure 2.** Schematic diagrams of the photobioreactor with moving media (MBPBR) and photobioreactor without moving media (SPBR) used in this study.

2.2.1. SBR Operation

Wastewater-borne algal–bacterial consortia ($400 \pm 15$ mg TSS·L$^{-1}$) were inoculated into the MBPBR and SPBR containing 12.5 L of wastewater and cultivated at 25 °C. The fill, react, and draw modes were sequenced in a 24 h cycle, with each cycle consisting of 5 min of filling with 5 L of domestic wastewater, 23 h and 50 min of reaction time, and 5 min of withdrawal. Thus, the HRTs of both reactors were 2.5 d. Mixed liquor suspended solids (MLSSs) were placed in a separate sedimentation vessel for 1 h, and the supernatant was used for physicochemical analysis.

2.2.2. Batch Operation

To evaluate the dynamics of nutrient removal by algal–bacterial consortia in the presence of moving media, the SPBRs were operated in batch mode for 24 h. The algal–bacterial consortium was grown in SBR operation mode using raw wastewater and used for batch testing on day 41 of the SBR operation. The experiments were conducted in the MBPBR and SPBR with 5 L of raw wastewater. Mixed liquor sampled every 2 h for 24 h was filtered using a GF/C glass microfiber filters (Whatman international Ltd., Maidstone, UK), and then the dynamics of nutrient removal were evaluated by physicochemical analysis. All the samples were taken in duplicate.

*2.3. Analytical Method*

2.3.1. Evaluation of the Performance of the MBPBR–SPBR

Evaluation of the performance of the MBPBR–SPBR was conducted by comparing the water quality indexes in the effluent. Regular parameters including biochemical oxygen demand (BOD$_5$), TN, NH$_3$-N, NO$_x{}^-$-N (NO$_2{}^-$-N + NO$_3{}^-$-N), TP, and photosynthetic oxygen production were selected as reference parameters. DO was measured using a calibrated YSI 5100 DO meter (Yellow Springs, OH, USA). Conductivity, pH, and water temperature were measured using a multipurpose water quality analyzer (YSI 550, YSI, Yellow Springs, OH, USA). An automated water analyzer (AASU2000, BLTEC, Japan) was used to measure the concentration of NH3-N, TKN, NOx–N, TN, and TP. Total biochemical oxygen demand (TBOD$_5$), carbonaceous biochemical oxygen demand (CBOD$_5$), and TSS were measured following the standard methods [22]. Attached biomass was determined by the difference in weight of 100 carriers before and after removing the biomass by washing. In this procedure, 3 h sonification was performed with a 6% NaOCl, while rinse step was carried out in every hour with the chlorinated solution and a final rinse with de-ionized water. This was conducted twice before and after each set of experiments. There was no significant difference in the amount of attached biomass. Algal–bacterial consortium was filtered with GF/C glass microfiber filters (Whatman international Ltd., Maidstone, UK) and then chlorophyll-*a* concentration was determined by extracting pigments in 10 mL of 90% (*v/v*) acetone and measuring the absorbance using a spectrophotometer (UV-2100, Shimadzu, Kyoto, Japan) at 630, 645, 663, and 750 nm [23]. The microalgal species were identified and classified using light microscopy (Axioskop 2 plus, Zeiss, Germany) [24]. Light intensities were measured using a Delta OHM photo-radiometer (HD 2102, Delta OHM, Padova, Italy). Concentration of microalgal biomass was estimated by assuming that the microalgae contained 1.5% (*w/w*) chlorophyll-*a* [25]. Although there is some debate regarding evaluating microalgae biomass from the concentration of chlorophyll-*a*, it is widely regarded as a practical method [26].

2.3.2. Mass Balance

To evaluate the mass balance in both the MBPBR and SPBR, the TN and TP contents within the biomass were measured. For measuring TN and TP content, a modified standard Kjeldahl method [27] and colorimetric determination of phosphorus [28] were used,

respectively. The mass balance of nitrogen in the MBPBR and SPBR systems is given by Equation (1), which is a minor modification of an equation from Zimmo et al. [29].

$$Q_{\text{Inf}}(N)_{\text{Inf}} = Q_{\text{Eff}}(N)_{\text{Eff}} + N_{\text{Was}} + N_{\text{Av}} + N_{\text{Denit}} + N_{\text{unAcc}} \tag{1}$$

where $Q_{\text{Inf}}$ and $Q_{\text{Eff}}$ are the respective inflow and outflow (L·d$^{-1}$), $(N)_{\text{Inf}}$ and $(N)_{\text{Eff}}$ are the respective influent and effluent TN concentrations (mg N·L$^{-1}$), $N_{\text{Was}}$ is the nitrogen leaving the system by wastage of biomass containing synthesized or bio-adsorbed nitrogen (mg N·L$^{-1}$), $N_{\text{Av}}$ is the nitrogen leaving the system by ammonia volatilization (mg N·L$^{-1}$), $N_{\text{Denit}}$ is the nitrogen leaving the system by denitrification (mg N·L$^{-1}$), and $N_{\text{unAcc}}$ is the unaccounted fraction of nitrogen (mg N·L$^{-1}$). The mass balance of phosphorus in the MBPBR and SPBR systems is given by Equation (2), as follows:

$$Q_{\text{Inf}}(P)_{\text{Inf}} = Q_{\text{Eff}}(P)_{\text{Eff}} + P_{\text{Was}} + P_{\text{unAcc}} \tag{2}$$

where $Q_{\text{Inf}}$ and $Q_{\text{Eff}}$ are the respective inflow and outflow (L·d$^{-1}$), $(P)_{\text{Inf}}$ and $(P)_{\text{Eff}}$ are the respective influent and effluent total phosphorus concentrations (mg P·L$^{-1}$), $P_{\text{Was}}$ is the phosphorus leaving the system by wastage of biomass containing synthesized or bio-adsorbed phosphorus (mg P·L$^{-1}$), and $P_{\text{unAcc}}$ is the unaccounted fraction of phosphorus (mg P·L$^{-1}$). For the mass balance of nitrogen and phosphorus, when the water quality index in the effluent was stable after 10 d of operation, the mean concentrations of nitrogen and phosphorus in the biomass were estimated.

### 2.3.3. Settling Removal Efficiency and Biomass Recovery Rate

The algal–bacterial consortia biomass was settled in a gravimetric cell (10 mm × 10 mm × 50 mm) for 6 h. The harvesting efficiency was calculated using the optical density taken 25 mm below the top of the gravimetric cell. The optical density was measured at 490 mm for 6 h. The algae removal efficiency (RE) was calculated by measuring the optical density at time zero and after 1 h of settling using the following equation [30]:

$$\text{RE} = [1 - \left( \frac{O.D._f}{O.D._{t_0}} \right)] \times 100 \tag{3}$$

where $O.D._f$ is the optical density after 1 h of settling and $O.D._{t_0}$ is the initial optical density at time zero.

The biomass recovery rate was calculated by measuring the optical density continuously at 490 nm for 6 h using the following equation:

$$\text{Recovery rate (\%)} = [\frac{O.D._{t_0} - O.D._t}{O.D._{t_0}}] \times 100 \tag{4}$$

where $O.D._t$ is the optical density at time $t$ and $O.D._{t_0}$ is the initial optical density at time zero.

### 2.4. Community Analysis by NGS

Two MLSS samples were collected from the MBPBR and SPBR 30 d after operation. For bacterial community analysis, Deoxyribonucleic acid (DNA) was extracted from these samples, and emulsion-based polymerase chain reaction (PCR) (emPCR) and next-generation sequencing were conducted as described previously [7]. Briefly, the extracted bacterial genomic DNA was used for PCR amplification. To amplify the 16S ribosomal Ribonucleic acid (16s rRNA) gene of bacteria, the bacterial universal primers 27F (5′ GAGTTTGATCMTG-GCTCAG 3′) and 800R (5′ TACCAGGGTATCTAATCC 3′) were used. Fast Start High Fidelity PCR system (Roche, Indianapolis, IN, USA) was used for PCR. The emPCR was performed using a GS-FLX+ emPCR Kit (454 Life Sciences, Branford, CT, USA). The experiments were repeated at least three times. Subsequent sequencing was performed by Macrogen (Seoul, Korea).

### 2.5. Statistics

All analytical determinations were performed in triplicate unless otherwise specified. The data showed the mean and standard deviation of all the samples. The unpaired Student's *t*-test ($\alpha$ = 0.05) was used to calculate the statistical significance (*p* values) of the results.

## 3. Results and Discussion

### 3.1. Cultivation and Photosynthetic Oxygen Production

The operational parameters of each reactor during the steady-state period, such as the HRT (2.5 d for MBPBR and SPBR), temperature (16.9 °C and 16.9 °C, respectively), pH (7.4 and 7.4, respectively), and conductivity (484.3 $\mu S\cdot cm^{-1}$ and 611.7 $\mu S\cdot cm^{-1}$, respectively), are listed in Table S1.

The biomass concentrations in each reactor, including suspended and attached growth, were measured (Table 1). Considering the suspended biomass, the biomass curves (MLSS) for the MBPBR and SPBR during the 41 operating days are shown in Figure 3A. Similar growth of algal–bacterial consortia was observed for suspended biomass; the mean concentrations of MLSS were 433.0 $\pm$ 110.8 mg·L$^{-1}$ and 449.5 $\pm$ 132.1 mg·L$^{-1}$ for the MBPBR and SPBR, respectively, thereby indicating that the moving media within the MBPBR did not influence the growth of suspended biomass compared with that of the SPBR. However, the total biomass in the MBPBR had a higher concentration of 617.9 mg·L$^{-1}$ compared with that of 449.5 mg·L$^{-1}$ in the SPBR, even if the packing rate of the moving media was 5% in the MBPBR, thereby indicating that a large part of the biomass was attached to the moving media (Table 1). Meanwhile, MBPBR was more resistant to the temperature than SPBR. As the temperature decreased, it was observed that algae growth and the amount of photosynthetic oxygen decreased, thus, supplementary aeration might be needed. However, it was observed that microalgae attached to media could grow at 13 °C in this study.

**Table 1.** Biomass concentrations and photosynthetic oxygen production of the photobioreactor (PBR) with a moving bed (MBPBR) and PBR without a moving bed (SPBR).

| | | MBPBR | SPBR |
|---|---|---|---|
| Suspended growth | mg TSS·L$^{-1}$ | 433.0 $\pm$ 110.8 | 449.5 $\pm$ 132.1 |
| Attached growth | mg TSS·L$^{-1}$ | 4132.4 $\pm$ 39.6 | - |
| | mg TSS·L$^{-1}$ [a] | 617.9 $\pm$ 105.2 | 449.5 $\pm$ 132.1 |
| | mg Chl-*a*·L$^{-1}$ | 4.28 $\pm$ 1.01 | 2.24 $\pm$ 0.91 |
| Suspended + attached growth | mg algae·L$^{-1}$ [b] | 285.43 $\pm$ 65.12 | 149.25 $\pm$ 60.83 |
| | % algae | 41.35 $\pm$ 8.99 | 35.30 $\pm$ 14.80 |
| | mg DO·L$^{-1}$ | 5.9 $\pm$ 2.5 | 0.4 $\pm$ 0.1 |

[a] The total biomass was calculated using the packing ratio of the moving media (5%). [b] The algal biomass concentration (mg algae·L$^{-1}$) was calculated from the chlorophyll-*a* (Chl-*a*) concentration, as follows [25]: algal biomass (mg·L$^{-1}$) = 100/1.5 × Chl-*a* (mg·L$^{-1}$). Total Suspended Solid (TSS). Dissolved Oxygen (DO).

As the 5L MLSS d$^{-1}$ was wasted from MBPBR and SPBR, the mean biomass productivity was 17.32 $\pm$ 4.43 g·m$^{-2}$·d$^{-1}$ and 17.98 $\pm$ 5.28 g·m$^{-2}$·d$^{-1}$, respectively.

In similar experiments with SPBRs, these values were higher than those reported by previous studies, in which a biomass productivity of 10.9 $\pm$ 1.1 g·m$^{-2}$·d$^{-1}$ was observed in an SPBR illuminated by two compact fluorescent lamps with 360 $\mu mol\cdot m^{-2}\cdot s^{-1}$ for a period of 12 h/d and operated at an HRT of 8 d [31]. The higher biomass productivity in our study might have been caused by the short HRT of 2.5 d.
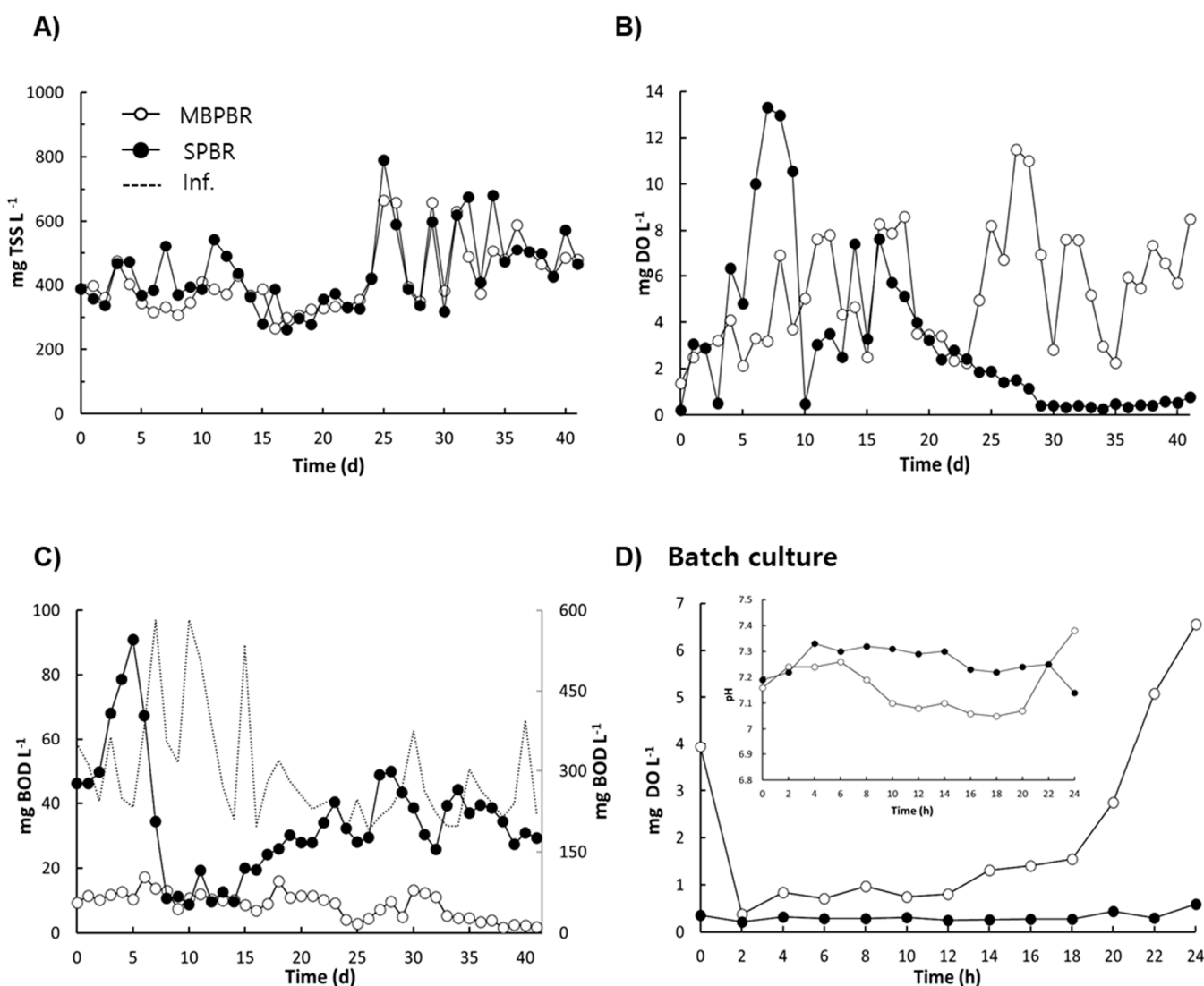
**Figure 3.** Daily variation in the effluent concentrations of suspended-growth biomass (**A**), dissolved oxygen (DO) (**B**), and biological oxygen demand (BOD) (**C**) from photobioreactors (PBRs) for the operating days. Temporal variation in the effluent concentration of DO and pH from PBRs for 24 h (**D**). MBPBR and SPBR represent the PBR with a moving bed and the PBR without a moving bed at light intensities of 500 $\mu mol \cdot m^{-2} \cdot s^{-1}$, respectively. Both the MBPBR and SPBR were operated with a hydraulic retention time of 4 d. Measurements were conducted in triplicate and the mean values of the triplicates were plotted. Total Suspended Solid (TSS).

The photosynthetic oxygen production of algal bacterial consortia is also an important consideration for algae-based wastewater treatment. The effect of moving media on DO is shown in Figure 3B. The mean concentration of DO was maintained at $5.9 \pm 2.5$ mg·L$^{-1}$ for the MBPBR. In contrast, the concentration of DO significantly decreased after 16 d and was approximately 0.2 mg·L$^{-1}$ for the SPBR. For the SPBR, a significant decrease in DO (0.2 mg·L$^{-1}$) was clearly observed when the concentration of biomass was over 600 mg TSS·L$^{-1}$ of suspended growth (Figure 3A,B). Kang et al. (2018) reported that DO concentrations in the reactors were nearly 0.0 mg $O_2$·L$^{-1}$ when the SPBRs were operated at 700–900 mg TSS·L$^{-1}$ of suspended growth [7]. For the MBPBR, although a high biomass concentration, which showed over 433 mg TSS·L$^{-1}$ of suspended growth plus 4132 mg TSS·L$^{-1}$ of attached growth, was maintained, the concentration of DO was over 3.0 mg·L$^{-1}$, thereby indicating that the microalgae in the moving media enhanced the photosynthetic oxygen production in the MBPBR.

The net result of the DO concentration, namely, photosynthetic oxygen minus oxygen consumption, indicated that low concentrations of DO resulted in insufficient photosynthetic oxygen production and high oxygen consumption. As shown in Figure 3C, the mean concentrations of BOD decreased from $282.08 \pm 100.60$ mg·L$^{-1}$ in the influent to $7.75 \pm 3.92$ mg·L$^{-1}$ (97.2% removal) and $29.89 \pm 10.83$ mg·L$^{-1}$ (88.0% removal) in the effluent for the MBPBR and SPBR, respectively, thereby indicating that photosynthetic oxygen was not sufficient to induce sufficient organic removal in the SPBR but was sufficient to compensate for oxygen consumption such as organic removal and nitrification in the MBPBR.

To investigate the patterns of DO and pH over time, a batch culture was performed at 41 d post-operation (Figure 3D). Zhang et al. (2016) reported that the turning points and plateaus of the pH and DO profiles indicated the end of biochemical reactions such as BOD consumption, ammonia oxidation, and denitrification [32]. For the MBPBR, there were three turning points; the initial concentration of DO decreased from 3.9 mg·L$^{-1}$ to 0.2 mg·L$^{-1}$ for 2 h, which was followed by a gradual increase to 1.6 mg·L$^{-1}$ until 18 h and then a significant increase to 6.6 mg·L$^{-1}$ for 6 h post-operation, thereby suggesting that the initial decrease in DO might have been caused by the initial BOD consumption and the gradual decrease in DO might have been due to the nitrification until 18 h. Meanwhile, for the pattern of pH in the MBPBR, changes in the initial increase, gradual decrease, and rapid increase were observed over time. The initial increase in pH might have been the result of intensive $CO_2$ utilization by algal growth, and the gradual decrease in pH might have been due to nitrification. The rapid increase in DO coordinated well with the rapid increase in pH at 18 h for the batch culture of the MBPBR, thereby indicating that algal growth might have induced a rapid increase in DO when the BOD consumption and nitrification reaction were completed, and the increase in pH was the result of nitrate uptake and $CO_2$ consumption during photosynthesis. For the SPBR, the DO concentration was maintained at approximately 0.3 mg·L$^{-1}$, and an initial increase and then a gradual decrease in pH were observed during 24 h, thereby indicating that biochemical reactions such as BOD consumption and nitrification did not end. Thus, it is important to consider photosynthetic oxygen and pH for the removal of heterotrophic organic material, and possibly nitrogen, when considering cultivation of algal–bacterial consortia using real wastewater. Moreover, the results displayed in Figure 3 demonstrate that moving media enhanced the photosynthetic oxygen production and organic removal in the PBR even under high biomass conditions (>600 mg TSS·L$^{-1}$).

### 3.2. Nutrient Removal

Short HRTs are usually considered to advance the engineering of cost-effective algae-based wastewater treatment. In this study, moving media could enhance the nutrient removal of the PBR with an HRT of 2.5 d. As shown in Figure 4A–C, 10 d after starting the reactor, the concentrations of TN, ammonia, and nitrate in the effluent were stabilized in the MBPBR. A preliminary statistical analysis ($p < 0.05$) showed that the MBPBR had statistically higher nitrogen removal rates than the SPBR. The mean concentrations of TN decreased from $65.98 \pm 9.13$ mg·L$^{-1}$ in the influent to $24.80 \pm 4.11$ mg·L$^{-1}$ (61.6% removal) for the SPBR and to $8.13 \pm 2.31$ mg·L$^{-1}$ (87.7%) for the MBPBR (Table S2), thereby indicating that the assimilation of ammonia and nitrate was more activated in the MBPBR than in the SPBR because the algal biomass concentration was higher in the MBPBR than in the SPBR. Xin et al. (2010) reported that microalgae could remove nitrogen with nitrate as a nitrogen source (90% nitrogen removal) and ammonia as a nitrogen source (31.1%) owing to the inhibitory effect of the algal culture's acidic pH caused by H$^+$ release from $NH_4^+$ during the algal cultivation process [33]. Thus, the higher TN removal and DO concentration observed in the MBPBR suggested that nitrification might be more activated in the MBPBR than in the SPBR. The results displayed in Figure 4B–E demonstrate that nitrification was activated not in the SPBR, but in the MBPBR. The mean concentration of NH$_3$-N decreased from $33.10 \pm 4.76$ mg·L$^{-1}$ in the influent to $1.62 \pm 1.92$ mg·L$^{-1}$ (95.3% removal) and

$21.34 \pm 3.92$ mg·L$^{-1}$ (33.8%) in the effluent of the MBPBR and SPBR during the operating days, respectively (Figure 4B). Furthermore, the mean concentrations of NO$_x{}^-$-N in the effluent were $6.18 \pm 1.89$ mg·L$^{-1}$ and $0.48 \pm 0.64$ mg·L$^{-1}$ for the MBPBR and SPBR during the operating days, respectively, thereby indicating that nitrification was clearly detected in the MBPBR (Figure 4C). As shown in Figure 4D,E, the decrease in ammonia (from 9.6 mg NH$_3$-N·L$^{-1}$ at 4 h to 0.0 mg NH$_3$-N·L$^{-1}$ at 22 h) coordinated well with the increase in nitrate (from 0.6 mg NO$_3{}^-$-N·L$^{-1}$ at 4 h to 4.6 mg NO$_3{}^-$-N·L$^{-1}$ at 22 h). The nitrogen difference (5.0 mg N·L$^{-1}$) obtained by subtracting NO$_3{}^-$-N (4.6 mg NO$_3{}^-$-N·L$^{-1}$) from NH$_3$-N (9.6 mg NH$_3$-N L$^{-1}$) was the result of ammonium and nitrate uptake in microalgae. Moreover, the fact that microalgae could absorb ammonium and nitrate well in the MBPBR suggested that algae-based wastewater treatment could be beneficial for nitrogen removal because of the reduction in the nitrogen load for denitrification.

However, an initial decrease in nitrate (from 3.2 mg NO$_3{}^-$-N·L$^{-1}$ to 0.6 mg NO$_3{}^-$-N·L$^{-1}$ for 4 h) was detected in the batch culture of the MBPBR (Figure 4E). As the initial pH also increased at this time (Figure 3D), both nitrate uptake and denitrification could be possible explanations for the phenomenon. However, considering the competition between ammonia and nitrate for substrate as a nitrogen source in microalgae, Kang et al. (2018) reported that the diauxic growth of wastewater-borne algal–bacterial consortia using real wastewater showed an initial uptake of ammonia, a lag phase, and then post-uptake of nitrate under similar experimental conditions [7]. Thus, it can be assumed that the initial decrease in nitrate in the MBPBR for 4 h displayed in Figure 4E might have been caused not by nitrate uptake, but by denitrification due to the presence of moving media. This hypothesis was verified by the results of the nitrogen mass balance (Figure 4F). The TN contents of MLSS of $7.1 \pm 0.2$% (*w/w*) and $8.2 \pm 0.2$% (*w/w*) for the MBPBR and the SPBR, respectively, indicated that the amount of nitrogen leaving the system by nitrogen assimilation was 152.8 mg N·d$^{-1}$ (46.4%) and 183.6 mg N·d$^{-1}$ (55.7%) for the MBPBR and the SPBR, respectively. The amount of nitrogen leaving the system by effluent was 40.4 mg N·d$^{-1}$ (12.3%) for the MBPBR and 123.1 mg N·d$^{-1}$ (37.6%) for the SPBR. Thus, the amount of additional nitrogen leaving the system was 136.2 mg·d$^{-1}$ (41.3%) and 22.7 mg·d$^{-1}$ (6.8%) for the MBPBR and the SPBR, respectively. As possible nitrogen removal mechanisms are usually described as cell assimilation and denitrification, additional nitrogen leaving the system was the result of denitrification. Ammonia stripping, an abiotic process, was disregarded as the pH of both reactors was maintained at $7.2 \pm 0.4$. Thus, it was reasonable to conclude that the main mechanisms of nitrogen removal were denitrification and cell synthesis for the MBPBR and cell synthesis for the SPBR. Therefore, it can be suggested that denitrification and cell synthesis might be essential processes for increasing the nitrogen removal in PBRs using real wastewater, which could be enhanced by using moving media.

Phosphorus removal in these reactors was also investigated. As displayed in Figure S1A,B, the decrease in phosphorus was more clearly detected from the MBPBR within 41 d and from the batch culture within 24 h compared with that in the SPBR; the mean concentration of phosphorus decreased from $7.00 \pm 1.18$ mg·L$^{-1}$ in the influent to $0.77 \pm 0.40$ mg·L$^{-1}$ (88.7% removal) and $2.24 \pm 0.88$ mg·L$^{-1}$ (66.4% removal) in 41 d for the MBPBR and SPBR, respectively. The batch culture showed that the concentration of phosphorus decreased from $2.49 \pm 0.21$ mg·L$^{-1}$ to $0.98 \pm 0.14$ mg·L$^{-1}$ for the MBPBR and from $3.17 \pm 0.34$ mg·L$^{-1}$ to $2.60 \pm 0.23$ mg·L$^{-1}$ for the SPBR in 24 h. Previous studies have shown that wastewater-borne algal–bacterial consortia had phosphate REs from municipal wastewater ranging from 54.5% to 72.6% [31]. One possible explanation for the distinct superiority of phosphorus removal in the MBPBR might be the increased phosphorus accumulation into biomass caused by moving media, with 617.9 mg TSS·L$^{-1}$ for the MBPBR and 449.5 mg TSS·L$^{-1}$ for the SPBR. Phosphorus can be removed by both biotic phosphorus accumulation into biomass and abiotic phosphorus precipitation at a high pH (9–11) [34]. In both PBRs, abiotic phosphorus precipitation was not performed because the pH of the PBRs was maintained at $7.4 \pm 0.4$. The phosphorus mass balance based on 41 working days

is displayed in Figure S1C. As phosphorus accumulation into biomass was still the main mechanism in both PBRs, the fact that wasted phosphorus totaled 31.8 mg·d$^{-1}$ (89.3%) in the MBPBR and 24.6 mg·d$^{-1}$ (69.1%) in the SPBR also suggested that moving media enhanced the phosphorus accumulation into biomass. Su et al. (2011) also reported that phosphorus accumulation in biomass ranged from 50.1% to 67.1%. Therefore, bio-P organisms might be more dominant in MBPBRs than SPBRs owing to the moving media [31].
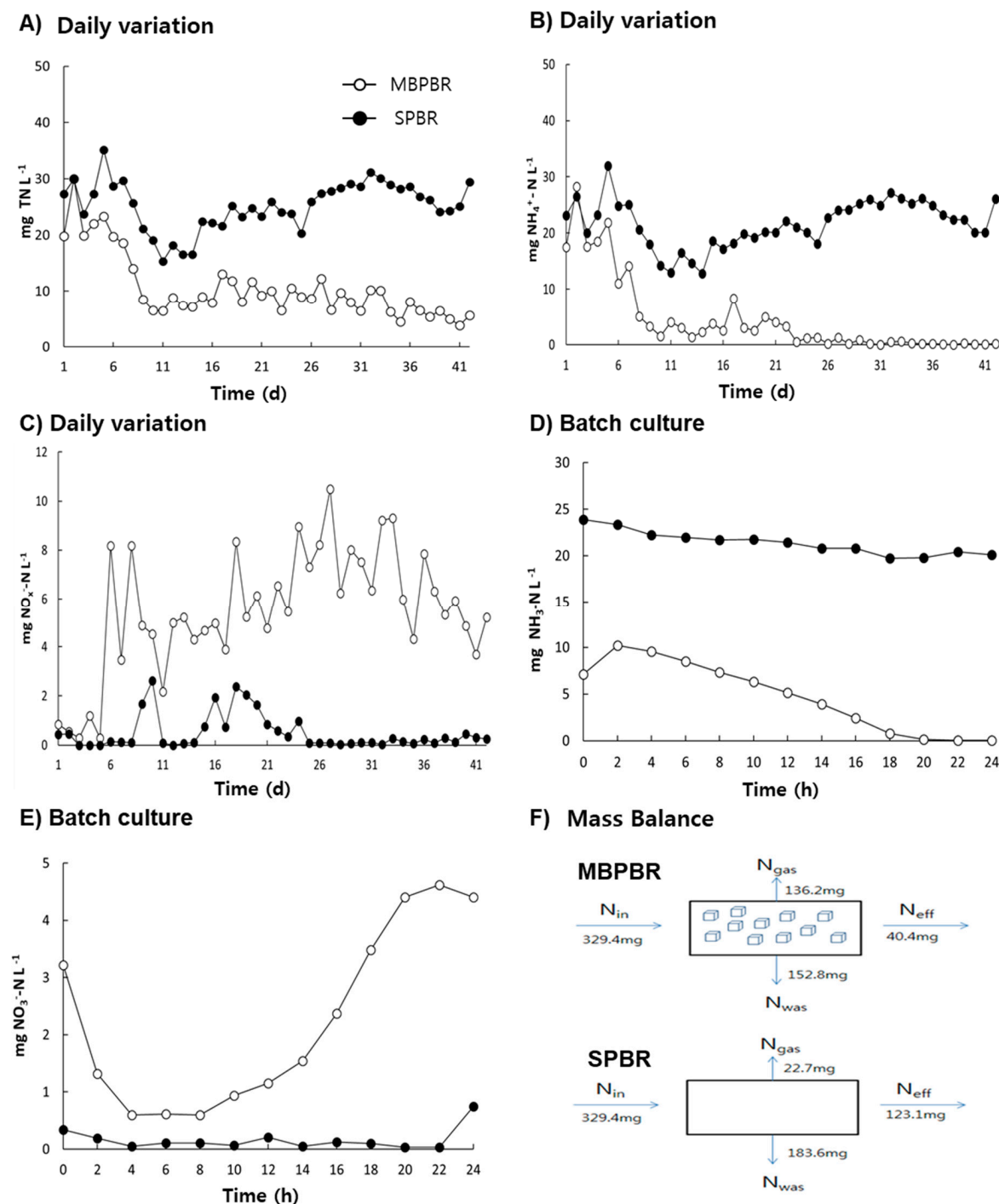


**Figure 4.** Daily variation in the effluent concentrations of total nitrogen (TN) (**A**), ammoniacal nitrogen (NH$_3$-N) (**B**), and NO$_x^-$-N (sum of NO$_2^-$-N and NO$_3^-$-N) (**C**) from the photobioreactors (PBRs) during the operating days. Temporal variation in the effluent concentrations of NH$_3$-N (**D**) and NO$_x^-$-N (**E**). Mass balance of nitrogen in the PBR with a moving bed (MBPBR) and PBR without a moving bed (SPBR) during the operating days (**F**). Measurements were conducted in triplicate and the mean values of the triplicates were plotted.

### 3.3. Settling Effect

Cost-effective harvesting of algal–bacterial consortia is crucial in wastewater treatment, together with the problematic area of stabilization of oxidation ponds [35]. Although many separation methods, such as centrifugation, filtration, flocculation, increasing salinity, and flotation, have been developed for microalgae recovery [36,37], to our knowledge, few studies have reported the settling effect of algal–bacterial consortia induced by moving media. As shown in the recovery efficiency curves (Figure 5), a clear settling effect was observed from the biomass of the MBPBR compared with that of the SPBR. The algae REs were 71.15 ± 0.70% and 20.59 ± 0.72% after 1 h for the MBPBR and the SPBR (data not shown), respectively, thereby indicating that the attached growth of algal–bacterial consortia might have enhanced the settling effect more than the suspended growth of algal–bacterial growth. There are two possible explanations for this phenomenon. First, algal–bacterial consortia with adherence characteristics may grow on the moving media and then exhibit stronger flocculation compared with that of suspended growth, even after leaving the moving media. Second, moving media might influence the algal and bacterial communities. The observation of algae species supported this hypothesis.
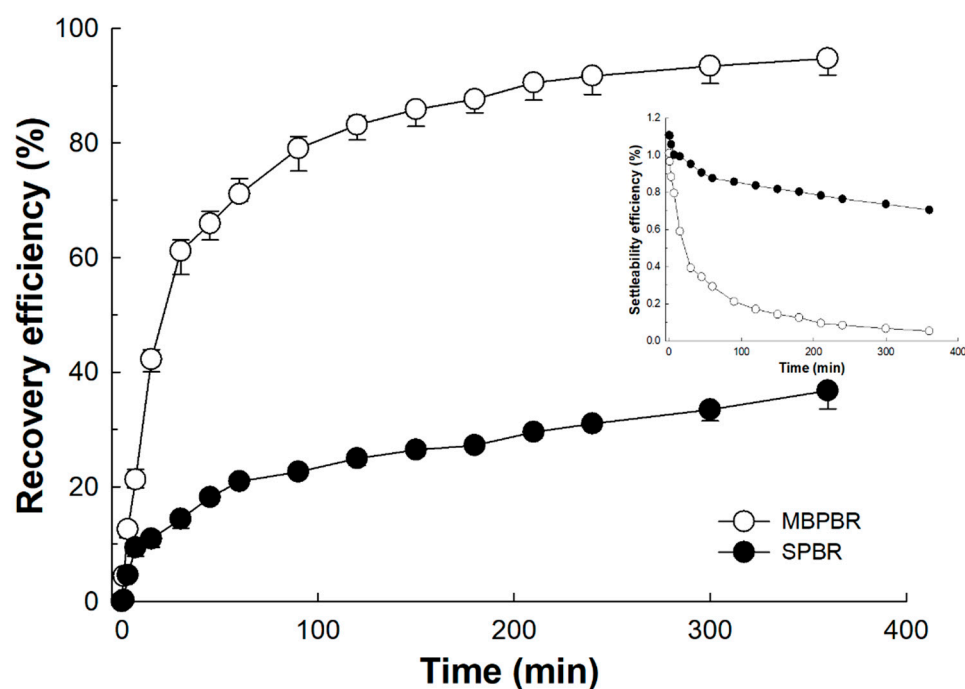


**Figure 5.** Settling effect of biomass from the photobioreactor with a moving bed (MBPBR) and the photobioreactor without a moving bed (SPBR). The recovery efficiency was calculated from the settleability efficiency with a continuous optical density of 490 nm for 6 h, as follows. Recovery efficiency (%) = $(O.D._{t0} - O.D._{t})/O.D._{t0} \times 100$, where $O.D._{t}$ is the optical density at time $t$ and $O.D._{t0}$ is the initial optical density at time zero. Measurements were conducted in triplicate and the mean values of the triplicates were plotted.

Although the unicellular green alga *Chlorella* sp. was the main species of algae in both PBRs, several species of algae were also detected from the surface of the moving media in the MPBR, but not in the SPBR (Figure 6A). The unicellular green alga *Chlorella* sp. showed fast initial growth and was easily dispersed without aggregation (data not shown). Meanwhile, the species of algae detected in the MBPBR were filamentous green algae, diatoms, and coherent unicellular *Scenedesmus.* sp. (data not shown). Henderson et al. (2008) examined the flocculation of freshwater algae (green algae, blue-green algae, and diatoms) for water treatment and concluded that the key properties that affect algal flocculation include cell morphology, surface charge density, cell concentration, mineral content, extracellular organic matter concentration, and composition [38]. Thus, the types of filamentous and

coherent microalgae might enhance the flocculation and settling ability of algal–bacterial consortia. In addition, the species diversity inducing these species of microalgae might be due to the existence of moving media.

### 3.4. Community Structure

As a common hypothesis, bacterial diversity in algae-based biological wastewater treatment may affect the performance of PBRs. However, it remains largely unstudied. Pyrosequencing using the 16S rRNA gene as the biomarker was performed to estimate the bacterial diversity of these PBR samples, compare the unique dominant bacterial populations, and identify the core populations shared by different samples. The 16S rRNA gene libraries were constructed and sequenced, yielding a total of 153,699 qualified reads. The operational taxonomic unit (OTU) numbers ranged from 1321 to 1527 in different samples, which were similar to the numbers of bacterial OTUs (from 1183 to 3567; 3% cutoff) in activated sludge from the USA, Canada, Hong Kong, and Singapore [39].

At the family level, the top 10 families in each sample are summarized in Table 2. These data showed clear dominant families in the MBPBR and the SPBR. Comamonadaceae, Rhodocyclaceae, Saprospiraceae, Sphingomonadaceae, and Xanthomonadaceae were the families found in both PBRs. The families of Anaerolineaceae, Alcaligenaceae, Caldilineaceae, Halomonadaceae, and Sinobacteraceae were more abundant in the MBPBR, whereas the families of Brucellaceae, Chlorobiaceae, Flavobacteriaceae, Moraxellaceae, and Nautiliaceae were more abundant in the SPBR. The bacterial community structure was significantly changed at the phylum level owing to the presence of moving media (Figure 6B). The phyla Proteobacteria, Bacteroidetes, Cyanobacteria, and Chloroflexi accounted for 40.83%, 19.86%, 16.56%, and 6.50% of the total for the MBPBR and 78.64%, 9.88%, 1.64%, and 1.17% of the total for the SPBR, respectively. The SPBR results were consistent with the report that the main bacteria present in a PBR illuminated by white light were $\gamma$-proteobacteria, Bacteroidia, $\beta$-proteobacteria, and Flavobacteria [31]. Moreover, although a few species of bacteria were significantly abundant in the SPBR, the diversity of the species distribution was clear in the MBPBR. Moraxellaceae and Rhodocyclaceae encompassed 46.77% of the families in the SPBR, and Proteobacteria and Bacteroidetes encompassed 88.52% of the phyla in the MBPBR. Therefore, moving media changed the bacterial community and enhanced the species distribution.

**Table 2.** Abundances of the top 10 families in each sample.

| MBPBR | Frequency of Family (%) | SPBR | Frequency of Family (%) |
|---|---|---|---|
| *Saprospiraceae* | 8.49 | *Moraxellaceae* | 29.14 |
| *Rhodocyclaceae* | 6.59 | *Rhodocyclaceae* | 17.63 |
| *Comamonadaceae* | 4.84 | *Comamonadaceae* | 8.45 |
| *Anaerolineaceae* | 3.79 | *Brucellaceae* | 4.71 |
| *Xanthomonadaceae* | 2.47 | *Nautiliaceae* | 1.71 |
| *Sinobacteraceae* | 2.28 | *Flavobacteriaceae* | 1.57 |
| *Sphingomonadaceae* | 2.02 | *Sphingomonadaceae* | 1.54 |
| *Halomonadaceae* | 1.82 | *Saprospiraceae* | 1.48 |
| *Caldilineaceae* | 1.75 | *Xanthomonadaceae* | 1.48 |
| *Alcaligenaceae* | 1.34 | *Chlorobiaceae* | 1.32 |

Taxonomic assignment of bacteria in the bioreactor at the family level shown as a percentage of the total microbiota.
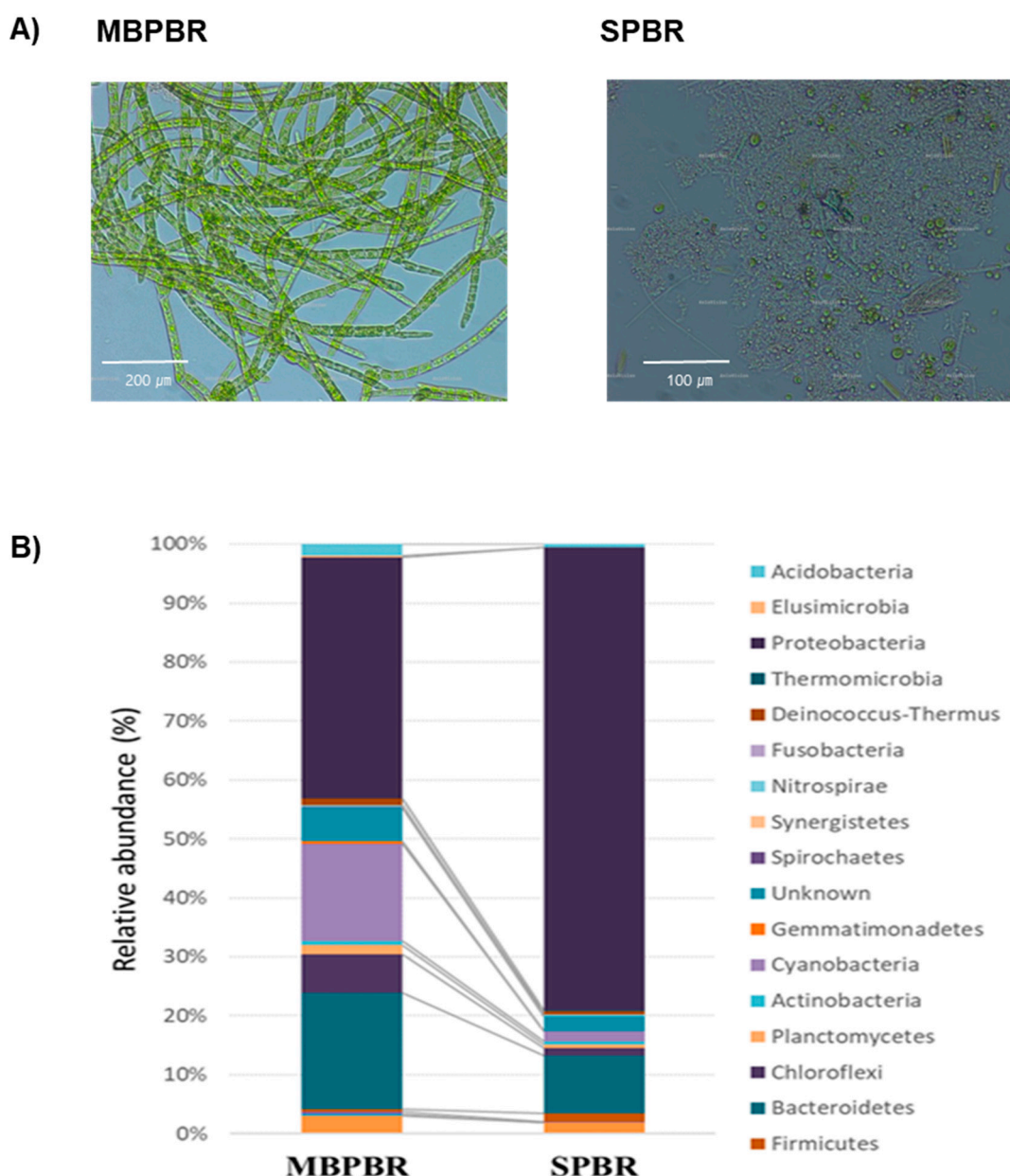
**Figure 6.** Biofloc of microalgae and other microbes from the photobioreactor with a moving bed (MBPBR) and the photobioreactor without a moving bed (SPBR) (**A**). Bacterial communities at the phylum level of the algal–bacterial consortia from the MBPBR and SPBR 30 d after operation (**B**). Phyla with a mean relative abundance greater than 0.01% are shown.

## 4. Conclusions

Under the conditions of an MBPBR with an HRT of 2.5 d, wastewater-borne algal–bacterial consortia were successfully used to treat real wastewater. Moving media enhanced the photosynthetic oxygen concentration (0.2 mg $DO \cdot L^{-1}$ to 5.9 mg $DO \cdot L^{-1}$), BOD removal (88.0% to 97.2%), $NH_3$-N removal (33.8% to 95.3%), TN removal (61.6% to 87.7%), TP removal (66.4% to 88.7%), algal growth (149.3 mg algae$\cdot L^{-1}$ to 285.4 mg algae$\cdot L^{-1}$), and settleability (20.6% to 71.2% algae RE) compared with those of an SPBR. Although biomass uptake was the main mechanism for nutrient removal in the SPBR, both biomass uptake and denitrification were the main mechanisms under the MBPBR. The bacterial community also changed under the moving media condition. Thus, moving media could be an essential parameter for PBRs with a short HRT to implement realistic goals of nutrient removal and settleability. Furthermore, it is expected that the amount of oxygen by air blower for

nitrification and the energy for oxidation of organic matter might be reduced in terms of energy concept.

**Supplementary Materials:** The following are available online at https://www.mdpi.com/2227-97 17/9/1/116/s1, Figure S1: Daily variation (A) and time variation (B) in the effluent concentration of TP from MBPBR and SPBRs for operating days and 24 h, respectively. Mass balance of nitrogen in MBPBR and SPBR during operating days (C). Measurements were carried out in triplicate and the mean values of the triplicates were plotted, Table S1: The operational parameters of MBPBR and SPBR during steady-state period, Table S2: Average values and removal percentage of TN, $NO_x{}^-$-N, $NH_3$-N, BOD, and TP in the influent and effluents from PBRs.

**Author Contributions:** Conceptualization: D.K. and K.K.; methodology: D.K. and K.K.; formal analysis: D.K. and K.K.; investigation: D.K.; resources: D.K. and K.K.; statistical analysis: D.K. and K.K.; writing—original draft preparation: D.K. and K.K.; writing—review and editing: K.K.; visualization: K.K.; supervision: K.K.; project administration: D.K. and K.K. All authors have read and agreed to the published version of the manuscript.

**Institutional Review Board Statement:** Not applicable.

**Informed Consent Statement:** Not applicable.

**Data Availability Statement:** Due to confidentiality agreements, supporting data can only be made available to bona fide researchers subject to a non-disclosure agreement.

**Conflicts of Interest:** The authors declare no conflict of interest.

## Abbreviations

HRT      Hydraulic retention time
PBR      Photobioreactor
SPBR      PBR without moving media
MBPBR      PBR with moving media
SBRs      Sequencing batch reactors

## References

1. Karya, N.; van der Steen, N.; Lens, P. Photo-oxygenation to support nitrification in an algal–bacterial consortium treating artificial wastewater. *Bioresour. Technol.* **2013**, *134*, 244–250. [CrossRef] [PubMed]
2. Åmand, L.; Olsson, G.; Carlsson, B. Aeration control—A review. *Water Sci. Technol.* **2013**, *67*, 2374–2398. [CrossRef] [PubMed]
3. Vergara, C.; Muñoz, R.; Campos, J.L.; Seeger, M.; Jeison, D. Influence of light intensity on bacterial nitrifying activity in algal-bacterial photobioreactors and its implications for microalgae-based wastewater treatment. *Int. Biodeterior. Biodegrad.* **2016**, *114*, 116–121. [CrossRef]
4. Bordel, S.; Guieysse, B.; Munoz, R. Mechanistic model for the reclamation of industrial wastewaters using algal− bacterial photobioreactors. *Environ. Sci. Technol.* **2009**, *43*, 3200–3207. [CrossRef] [PubMed]
5. Medina, M.; Neis, U. Symbiotic algal bacterial wastewater treatment: Effect of food to microorganism ratio and hydraulic retention time on the process performance. *Water Sci. Technol.* **2007**, *55*, 165–171. [CrossRef] [PubMed]
6. Muñoz, R.; Guieysse, B. Algal–bacterial processes for the treatment of hazardous contaminants: A review. *Water Res.* **2006**, *40*, 2799–2815. [CrossRef] [PubMed]
7. Kang, D.H.; Kim, K.T.; Jang, Y.H.; Moon, H.C.; Ju, D.J.; Jahng, D. Nutrient removal and community structure of wastewater-borne algal-bacterial consortia grown in raw wastewater with various wavelengths of light. *Int. Biodeterior. Biodegrad.* **2018**, *126C*, 10–20. [CrossRef]
8. Gray, N.F. *Biology of Wastewater Treatment*; World Scientific: Hong Kong, China, 2004.
9. Valigore, J.M.; Gostomski, P.A.; Wareham, D.G.; O'Sullivan, A.D. Effects of hydraulic and solids retention times on productivity and settleability of microbial (microalgal-bacterial) biomass grown on primary treated wastewater as a biofuel feedstock. *Water Res.* **2012**, *46*, 2957–2964. [CrossRef]
10. Oswald, W.J.; Gotaas, H.; Ludwig, H.F.; Lynch, V. Algae symbiosis in oxidation ponds: II. Growth characteristics of Chlorella pyrenoidosa cultured in sewage. *Sew. Ind. Wastes* **1953**, *25*, 26–37.

11. Tamer, E.; Amin, M.; Ossama, E.; Bo, M.; Benoit, G. Biological treatment of industrial wastes in a photobioreactor. *Water Sci. Technol.* **2006**, *53*, 117–125. [CrossRef]

12. Muñoz, R.; Jacinto, M.; Guieysse, B.; Mattiasson, B. Combined carbon and nitrogen removal from acetonitrile using algal–bacterial bioreactors. *Appl. Microbiol. Biotechnol.* **2005**, *67*, 699–707. [CrossRef] [PubMed]

13. Posadas, E.; Bochon, S.; Coca, M.; García-González, M.; García-Encina, P.; Muñoz, R. Microalgae-based agro-industrial wastewater treatment: A preliminary screening of biodegradability. *J. Appl. Phycol.* **2014**, *26*, 2335–2345. [CrossRef]

14. Anbalagan, A.; Schwede, S.; Lindberg, C.-F.; Nehrenheim, E. Influence of hydraulic retention time on indigenous microalgae and activated sludge process. *Water Res.* **2016**, *91*, 277–284. [CrossRef]

15. Arcila, J.S.; Buitrón, G. Microalgae–bacteria aggregates: Effect of the hydraulic retention time on the municipal wastewater treatment, biomass settleability and methane potential. *J. Chem. Technol. Biotechnol.* **2016**, *91*, 2862–2870. [CrossRef]

16. Woertz, I.; Feffer, A.; Lundquist, T.; Nelson, Y. Algae grown on dairy and municipal wastewater for simultaneous nutrient removal and lipid production for biofuel feedstock. *J. Environ. Eng.* **2009**, *135*, 1115–1122. [CrossRef]

17. Van Den Hende, S.; Beelen, V.; Bore, G.; Boon, N.; Vervaeren, H. Up-scaling aquaculture wastewater treatment by microalgal bacterial flocs: From lab reactors to an outdoor raceway pond. *Bioresour. Technol.* **2014**, *159*, 342–354. [CrossRef]

18. Sutherland, D.L.; Howard-Williams, C.; Turnbull, M.H.; Broady, P.A.; Craggs, R.J. Frequency of $CO_2$ supply affects wastewater microalgal photosynthesis, productivity and nutrient removal efficiency in mesocosms: Implications for full-scale high rate algal ponds. *J. Appl. Phycol.* **2015**, *27*, 1901–1911. [CrossRef]

19. Katarzyna, L.; Sai, G.; Singh, O.A. Non-enclosure methods for non-suspended microalgae cultivation: Literature review and research needs. *Renew. Sustain. Energy Rev.* **2015**, *42*, 1418–1427. [CrossRef]

20. Kermani, M.; Bina, B.; Movahedian, H.; Amin, M.; Nikaein, M. Application of moving bed biofilm process for biological organics and nutrients removal from municipal wastewater. *Am. J. Environ. Sci.* **2008**, *4*, 675.

21. Wang, X.J.; Xia, S.Q.; Chen, L.; Zhao, J.F.; Renault, N.J.; Chovelon, J.M. Nutrients removal from municipal wastewater by chemical precipitation in a moving bed biofilm reactor. *Process Biochem.* **2006**, *41*, 824–828. [CrossRef]

22. APHA-AWA-WEF. *Standard Methods for the Examination of Water and Wastewater*, 21st ed.; American Public Health Association: Washington, DC, USA, 2005.

23. Mu, R.-M.; FAN, Z.-Q.; PEI, H.-Y.; Yuan, X.-L.; Liu, S.-X.; Wang, X.-R. Isolation and algae-lysing characteristics of the algicidal bacterium B5. *J. Environ. Sci.* **2007**, *19*, 1336–1340. [CrossRef]

24. Park, J.; Lee., J.; Jang, S. *Secure the Voucher Specimens and Photographs of Micro-Algae in the Korean Peninsula-Finnal Report*; Daegu University: Tadgu Tae, Korea, 2010.

25. Raschke, R. Guidelines for assessing and predicting eutrophication status of small southeastern piedmont impoundments. In *EPA Region IV*; Environmental Services Division, Ecological Support Branch: Athens, GA, USA, 1993.

26. Gasol, J.M.; Duarte, C.M. Comparative analyses in aquatic microbial ecology: How far do they go? *Fems Microbiol. Ecol.* **2000**, *31*, 99–106. [CrossRef] [PubMed]

27. Bremner, J. Salicylic acid-thiosulfate modification on Kjeldahl method to include nitrate and nitrite. *Chem. Microbiol. Prop. Methods Soil Anal.* **1982**, *2*, 621–622.

28. Fiske, C.H.; Subbarow, Y. The colorimetric determination of phosphorus. *J. Biol. Chem.* **1925**, *66*, 375–400. [CrossRef]

29. Zimmo, O.R.; van der Steen, N.P.; Gijzen, H.J. Nitrogen mass balance across pilot-scale algae and duckweed-based wastewater stabilisation ponds. *Water Res.* **2004**, *38*, 913–920. [CrossRef]

30. Garzon-Sanabria, A.J.; Davis, R.T.; Nikolov, Z.L. Harvesting Nannochloris oculata by inorganic electrolyte flocculation: Effect of initial cell density, ionic strength, coagulant dosage, and media pH. *Bioresour. Technol.* **2012**, *118*, 418–424. [CrossRef]

31. Su, Y.; Mennerich, A.; Urban, B. Municipal wastewater treatment and biomass accumulation with a wastewater-born and settleable algal-bacterial culture. *Water Res.* **2011**, *45*, 3351–3358. [CrossRef]

32. Zhang, C.; Zhang, H.; Yang, F. Granulation of non-filamentous bulking sludge directed by pH, ORP and DO in an Anaerobic/Aerobic/Anoxic SBR. *Appl. Biochem. Biotechnol.* **2016**, *178*, 184–196. [CrossRef]

33. Xin, L.; Hu, H.Y.; Ke, G.; Jia, Y. Growth and nutrient removal properties of a freshwater microalga Scenedesmus sp. LX1 under different kinds of nitrogen sources. *Ecol. Eng.* **2010**, *36*, 379–381. [CrossRef]

34. De Godos, I.; Blanco, S.; García-Encina, P.A.; Becares, E.; Muñoz, R. Long-term operation of high rate algal ponds for the bioremediation of piggery wastewaters at high loading rates. *Bioresour. Technol.* **2009**, *100*, 4332–4339. [CrossRef]

35. Kaya, D.; Dilek, F.B.; Gökçay, C.F. Reuse of lagoon effluents in agriculture by post-treatment in a step feed dual treatment process. *Desalination* **2007**, *215*, 29–36. [CrossRef]

36. Lee, A.K.; Lewis, D.M.; Ashman, P.J. Energy requirements and economic analysis of a full-scale microbial flocculation system for microalgal harvesting. *Chem. Eng. Res. Des.* **2010**, *88*, 988–996. [CrossRef]

37. Church, J.; Hwang, J.-H.; Kim, K.-T.; McLean, R.; Oh, Y.-K.; Nam, B.; Joo, J.C.; Lee, W.H. Effect of salt type and concentration on the growth and lipid content of Chlorella vulgaris in synthetic saline wastewater for biofuel production. *Bioresour. Technol.* **2017**, *243*, 147–153. [CrossRef] [PubMed]

38. Henderson, R.; Parsons, S.A.; Jefferson, B. The impact of algal properties and pre-oxidation on solid–liquid separation of algae. *Water Res.* **2008**, *42*, 1827–1845. [CrossRef] [PubMed]

39. Zhang, T.; Shao, M.-F.; Ye, L. 454 Pyrosequencing reveals bacterial diversity of activated sludge from 14 sewage treatment plants. *Isme J.* **2012**, *6*, 1137–1147. [CrossRef] [PubMed]